Journal of Materials Chemistry C

From insulator to semiconductor: Effect of host-guest interactions on charge transport in M-MOF-74 metal-organic frameworks

Journal:	*Journal of Materials Chemistry C*
Manuscript ID	TC-COM-11-2023-004155.R1
Article Type:	Communication
Date Submitted by the Author:	31-Dec-2023
Complete List of Authors:	Angel, Sydney; California State University Chico, Chemistry and Biochemistry Barnett, Nicholas; California State University Chico; University of Illinois Chicago Foster, Michael; Sandia National Laboratories, Materials Chemistry Talin, A.; Sandia National Laboratories, Materials Physics; Sandia National Lab Stavila, Vitalie; Sandia National Laboratories, Engineered Materials Department, MS-9161 Allendorf, Mark; Sandia National Laboratory, So, Monica ; California State University Chico, Chemistry and Biochemistry

COMMUNICATION

From insulator to semiconductor: Effect of host-guest interactions on charge transport in M-MOF-74 metal-organic frameworks

Sydney M. Angel,[a] Nicholas S. Barnett,[a,b] A. Alec Talin,[c] Michael E. Foster,[c] Vitalie Stavila,[c] Mark D. Allendorf,[c] Monica C. So[a*]

[a] *Department of Chemistry and Biochemistry, California State University, Chico, Chico, CA 95973, United States. Email: mso@csuchico.edu Department of Physics, University of Illinois, Chicago, Chicago, IL, United States.*

[b] *Sandia National Laboratories, Livermore, CA 94551, United States.*

Electronic Supplementary Information (ESI) available: Procedures, materials, and instrumentation; characterization (PXRD, SEM, Raman, EA, UV, DRS, conductivity). See DOI: 10.1039/x0xx00000x

Received 00th January 20xx,
Accepted 00th January 20xx

DOI: 10.1039/x0xx00000x

Here, we report an air-free approach to infiltrate isostructural metal-organic frameworks (MOFs), M-MOF-74 (M = Cu, Mn, Zn, Mg), with conjugated acceptor, 7,7,8,8-tetracyanoquinodimethane (TCNQ). The TCNQ@M-MOF-74 compounds exhibit a striking correlation between their bulk conductivities and the open *d* shell variants (Cu, Mn), arising from TCNQ p-doping the MOFs. Importantly, conjugation of the guest molecule is a prerequisite for inducing electrical conductivity in these systems.

Combining the tunability and porosity of metal-organic frameworks (MOFs) with electronic (semi-)conductivity has driven the development of electronics, such as chemical sensors,[1–3] photovoltaics,[4–7] low-*k* dielectrics,[8,9] and non-volatile memory elements.[10] However, most existing MOFs are insulators due to the poor overlap between π orbitals of the organic linkers and *d* orbitals of the metal ions, suppressing charge transfer. By judiciously selecting metal ions with high-energy valence electrons and organic linkers that form coordination bonds with increased orbital delocalization between metal and linker, conductive MOFs have been realized.[6,11–14]

A paradigm-shifting alternative approach, which some of our team explored, successfully rendered the insulating $Cu_3(btc)_2$ MOF into an electrically conductive one by introducing a conjugated and redox-active guest molecule, 7,7,8,8-tetracyanoquinodimethane (TCNQ).[15] Since then, we also uncovered that the preferential ordering of the TCNQ molecules along the (111) lattice plane within HKUST-1 and the TCNQ bridging coordination motif to two adjacent copper paddlewheels facilitate conductivity.[16] Recently, others adapted this infiltration strategy for M-MOF-74 (M = Co,[1] Mn[17]) with densely packed open metal sites (OMS)[18–26] for effective host-guest interaction. To date, none have elucidated the nature of the host-guest complex or proposed conductivity mechanisms in the TCNQ@M-MOF-74 system. In general, the interaction between the guest and the host has been characterized as 'redox doping',[27,28] resulting in charge transfer and the formation of mobile charge carriers in the MOF conduction or valence bands and thus increased electrical conductivity.[29,30] However, these previous studies failed to address additional fundamental questions, such as: to what extent do open *d* shells of metal ions in M-MOF-74 influence charge transfer? What role does conjugation play in TCNQ in influencing electrical conductivity? How does oxygen affect the stability of TCNQ? Through what charge transport mechanism does TCNQ induce MOF conductivity?

These unanswered questions motivated us to closely scrutinize the nature of TCNQ@M-MOF-74 interactions that contribute to bulk conductivity. Recently, Bláha and colleagues confirmed charge transfer between TCNQ and Mn-MOF-74 by diagnostic Raman stretches, but their approach resulted in oxidized TCNQ.[17] Samples were further handled under ambient conditions, contaminating the host-guest system with oxygen. Our work expands upon their integral efforts, applying an air-free TCNQ infiltration approach into isostructural M-MOF-74, where M is divalent Mg, Mn, Cu, and Zn. Through rigorous exclusion of oxygen, our inert infiltration method yields no oxidized TCNQ. The coordination of TCNQ to the OMS of M-MOF-74 was confirmed by spectroscopy. Strikingly, we reveal that M-MOF-74 with open *d* shells and conjugated guest molecules are critical in forming charge transport networks, which are supported by temperature-dependent electrical conductivity measurements and density functional theory (DFT) calculations. Importantly, we propose a plausible mechanism to rationalize TCNQ binding to OMS of M-MOF-74 framework to form a continuous network. Together,

the experimental and theoretical results in this work shows that TCNQ p-dopes the M-MOF-74 (M = Cu, Mn) hosts, facilitating through-bond charge transport via conjugated TCNQ guests.

The powder x-ray diffraction (PXRD) scans confirm the identity of the M-MOF-74 (M=Cu, Mn, Zn, Mg) powders. PXRDs indicate M-MOF-74 are indeed isostructural, differing only differ by the metal ion (Figures 1a and S2). After TCNQ infiltration (Figures 1b-1e and S2), the MOFs not only remained crystalline but retained the same rough, porous morphology with some polycrystallinity. The presence of TCNQ in the MOFs was also confirmed by elemental analysis (Table S1). There are 2 TCNQs per cell of Cu-MOF-74 (1 TCNQ per 6 copper ions) and 4 TCNQs per cell of Mn-MOF-74 (2 TCNQ per 6 manganese ions). Importantly, there is no evidence of metal-containing TCNQ nanowires in the SEM data; these may form when TCNQ and M(II) are being reduced to $TCNQ^-$ and M(I) by oxidation.[16]

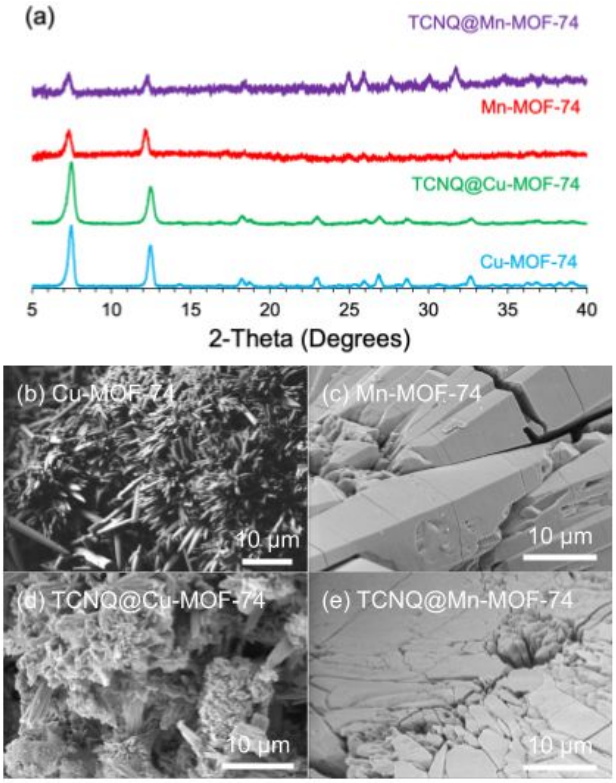

Figure 1. (a) PXRD of M-MOF-74 and TCNQ@M-MOF for M = Cu, Mn and SEM of (b) Cu-MOF-74, (c) Mn-MOF-74, (d) TCNQ@Cu-MOF-74, and (e) TCNQ@Mn-MOF-74.

To track the coordination of TCNQ to the OMS, Raman spectra were collected for TCNQ@M-MOF-74 (M=Cu, Mn). The frequencies of C=C and C≡N stretching modes of the TCNQ change depending on the degree of charge transfer in both MOF analogues. The 114 cm^{-1} mode shift of the C-CN wing stretch of TCNQ from 1462 to 1348 cm^{-1} indicate that TCNQ interacts with the OMS on the Cu^{2+} ions in Cu-MOF-74 (Figure 2a). The same shift occurs when TCNQ interacts with the OMS on the Mn^{2+} ions in Mn-MOF-74 (Figure 2b). A red shift of 19 cm^{-1} for the C=C wing stretching mode suggests a partial charge transfer of ~0.3 e^- between the framework and TCNQ.[31] The C≡N stretch at 2230 cm^{-1} indicates coordination of the TCNQ molecule to the metal ion for Cu-MOF-74 and Mn-MOF-74 (Figures 2a and 2b).

The C≡N stretch of TCNQ is also substantially broadened by adsorption for both analogues. Strikingly, the aforementioned signals are absent from Mg-MOF-74 and Zn-MOF-74 (Figures S4a and S4b), indicating the absence of TCNQ coordination.

With the TCNQ@M-MOF-74 (M = Cu, Mn) in hand, we performed UV-vis absorption and diffuse reflectance spectroscopies to evaluate intermolecular charge transfer. After TCNQ infiltration of Cu-MOF-74 and Mn-MOF-74, there is no band corresponding to the oxidation product of $TCNQ^{2-}$, dicyano-p-toluoyl cyanide, at 480 nm, as expected by eliminating oxygen during infiltration of the M-MOF-74 samples with TCNQ in the glovebox. Importantly, unlike the un-infiltrated MOF-74 samples, new lower energy absorption peaks appear at 660 and 800 nm (green, Figure 2c) and 850 nm (purple, Figure 2d), respectively. The strong 660 nm peak of TCNQ@Cu-MOF-74 is attributed to $TCNQ^{2-}$ formed by disproportionation of $TCNQ^-$ dimer, suggesting a salt of $[TCNQ]^{2-}[Cu\text{-}MOF\text{-}74]^{2+}$ formed.[1] The weaker absorption band at 800 nm for TCNQ@Cu-MOF-74 originates from the $TCNQ^-$ monomer.[27] The 850 nm peak in TCNQ@Mn-MOF-74 represents donor-acceptor charge transfer between the Mn-MOF-74 and confined TCNQ guests.[12] We also observe the optical band gaps decrease from 3.08 eV to 1.88 eV and from 2.48 eV to 1.46 eV, consistent with the formation of more conducting TCNQ@Cu-MOF-74 and TCNQ@Mn-MOF-74, respectively. These band gaps are comparable to those previously reported for TCNQ@Co-MOF-74 (1.5 eV)[1] and TNCQ@$Cu_3(btc)_2$ (1.76 eV).[15]

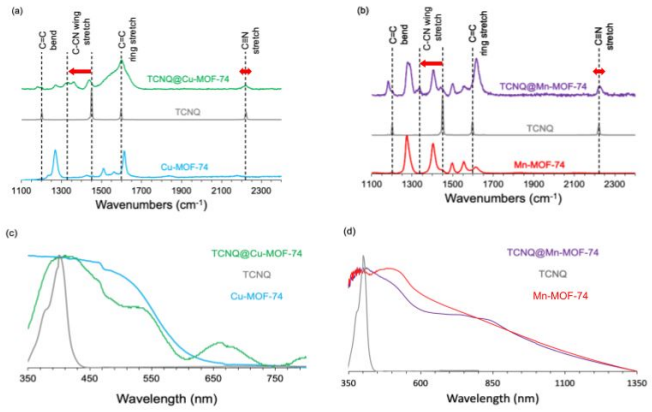

Figure 2. Raman spectra of (a) Cu-MOF-74 and (b) Mn-MOF-74 before and after TCNQ infiltration. (c) Transmission UV-Vis absorbance spectra of Cu-MOF-74 and (d) diffuse reflectance spectra of Mn-MOF-74 before and after TCNQ infiltration.

To determine the electronic conductivity, electrical transport measurements were performed on MOF pellets using a two-point probe geometry with large area electrodes to decrease the contact resistance. We used temperature-dependent measurements to extract the activation energy for electronic transport. Conductivity data gathered for all MOF pellets were at temperatures well below the MOF-74 thermal decomposition of 593 K.[1] We observe no detectable conductivity for TCNQ@M-MOF-74 (M = Mg, Zn) (Figure S5) as a function of increasing temperature, which is consistent with the lack of TCNQ coordination in these two variants. In contrast, as we increased the temperature from 294 K to 353 K for TCNQ@Cu-MOF-74 and TCNQ@Mn-MOF-74, their conductivity increased up to 5.40×10^{-2} $S \cdot m^{-1}$ and 5.02×10^{-3} $S \cdot m^{-1}$ with activation energies of

889.9 meV and 580.7 meV, respectively (Figure 3). These values are similar to those previously reported for TCNQ@Co-MOF-74.[1] Notably, the nonlinear activation energy of TCNQ@Cu-MOF-74 is attributed to the electron-electron Coulombic interactions of copper which varies by temperature. This interaction reduces the density of states near the Fermi level at lower temperatures (T<323 K in Figure 3c), thus increasing activation energy.[35] At T>323 K, lattice vibrations intensify, weakening electron binding in the outer layer of the atomic nucleus. Electrons likely move away from the nucleus, thus decreasing activation energy. [36]

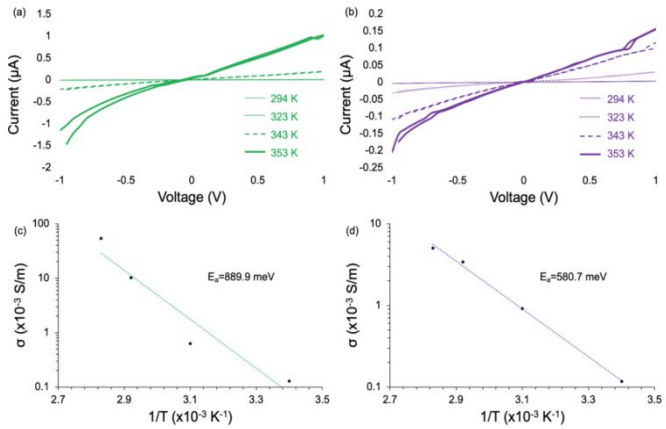

Figure 3. IV curves for (a) TCNQ@Cu-MOF-74 and (b) TCNQ@Mn-MOF-74, along with corresponding Arrhenius plots for (c) TCNQ@Cu-MOF-74 and (d) TCNQ@Mn-MOF-74.

To develop a deeper understanding of how TCNQ increases the electronic conductivity of Cu-MOF-74 and Mn-MOF-74, we performed DFT calculations. As illustrated in Figure 4a, the calculations indicate that TCNQ covalently binds to the OMS of the MOFs and that TCNQ molecules may form a new continuous network through the unit cell. Our calculations further show that the LUMO of TCNQ appears near the valence band of the MOFs (Figure 4b). For TCNQ@Cu-MOF-74, the LUMO of TCNQ slightly overlaps with the valence band of the MOF, as indicated by the blue/green shaded regions in Figure 4b. The resulting greater degree of overlap is consistent with the larger conductivity observed for the Cu variant compared to the Mn analogue (Figure 4c). Electron transfer from the MOFs to TCNQ is also predicted by Bader charge analysis (Table S2), suggesting that TCNQ p-dopes the MOFs in both analogues.

To further probe the effects of guest molecule on the formation of molecular pathways, we infiltrated the Cu and Mn versions of M-MOF-74 with the fully hydrogenated analogue of TCNQ, (cyclohexane-1,4-diylidene)dimalononitrile (H_4TCNQ). Elemental analysis indicates that the loading of H_4TCNQ is similar to that of TCNQ (i.e. 2 H_4TCNQ molecules per Cu-MOF-74 cell and 4 TCNQ molecules per Mn-MOF-74 cell). Although Raman suggests H_4TCNQ coordination to the OMS with a C-CN wing stretch shift and C≡N stretch broadening (Figures S4c and S4d), we observed that H_4TCNQ@M-MOF-74 (M = Cu, Mn) exhibit no detectable conductivity (Figures S6a and S6b). The same applies to the magnesium and zinc variants (Figures S6c and S6d). The crystals remained insulating, since the H_4TCNQ lacks a conjugated π electron network. Therefore, the presence of conjugation in the guest molecule is critical in completing the molecular network necessary for inducing conductivity in TCNQ@M-MOF-74, as was observed for TCNQ@$Cu_3(BTC)_2$.[15]

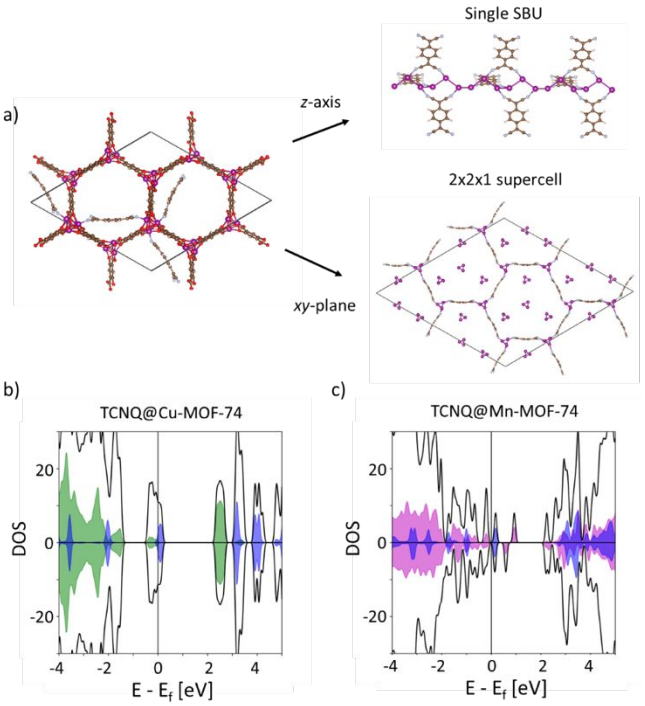

Figure 4. (a) Possible configuration predicted by DFT calculations of how TCNQ may provide continuous molecular networks through the M-MOF-74 unit cell. On the right, only the TCNQ and metal atoms are shown to illustrate the new channels in the z- (top) and xy-directions (bottom). In the HSE06 total and partial density of states for (b) TCNQ@Cu-MOF-74 and (c) TCNQ@Mn-MOF-74, the blue curve is the sum of states on the TCNQ molecule, and green/magenta curves are the Cu/Mn states, respectively.

In summary, we employed an air-free approach to infiltrate a series of isostructural M-MOF-74 (M = Cu, Mn, Zn, Mg) with TCNQ. This strategy produced no oxidized $TCNQ^{2-}$ by-product, unlike ambient infiltration strategy performed in previous studies. Infiltration of TCNQ into open *d* shell variants Cu-MOF-74 and Mn-MOF-74 yielded electrically conductive materials. Interestingly, the introduction of H_4TCNQ to the copper and manganese M-MOF-74 did not improve the conductivity, indicating the need for a conjugated π-network in the guest molecules to facilitate proper band alignment and thus charge transport. To our knowledge, this is the first work with computational evidence proposing an important structure-property relationship—binding of TCNQ to the OMS forms new molecular pathways and p-dopes the MOF-74 framework. Since most current conductive materials have limited chemical tunability, this work is an important step towards understanding how alternative charge transport pathways may help access conductive behavior in insulating inorganic parent materials. To guide future experimental efforts, computational analysis can determine what modifications make certain MOFs hold more metallic properties[29,30,32] or predict which MOFs will have lower bandgaps.[33] By fundamentally

understanding host-guest interactions, we can unlock the potential to transforming insulating materials into novel nanoporous conductive MOFs for electronic devices.[4,5,15,37–38]

M.C.S. acknowledges support from the National Science Foundation (CMMI-1920332, DMR-2137915), Camille and Henry Dreyfus Foundation (TH-23-035), and U.S. Department of Energy, Office of Science, Offices of Basic Energy Sciences and Electricity under contract DE-SC0024581. N.S.B. thanks CSU Chico's Lantis University Foundation. M.C.S. and S.M.A. are also grateful for support by the U.S. Department of Energy, Office of Science, Office of Workforce Development for Teachers and Scientists (WDTS), under the Visiting Faculty Program (VFP). Work at the Molecular Foundry was supported by the Office of Science, Office of Basic Energy Sciences, of the U.S. Department of Energy under Contract No. DE-AC02-05CH11231. Funding for this project was also provided by the Sandia Laboratory Directed Research and Development (LDRD) Program. AAT was supported by the Center for Reconfigurable Electronic Materials Inspired by Nonlinear Neuron Dynamics (reMIND), an Energy Frontier Research Center funded by the U.S. Department of Energy, Office of Science, Basic Energy Sciences. Sandia National Laboratories is a multimission laboratory managed and operated by National Technology and Engineering Solutions of Sandia, LLC, a wholly owned subsidiary of Honeywell International, Inc., for the U.S. Department of Energy's National Nuclear Security Administration under contract DE-NA-0003525. This paper describes objective technical results and analysis. Any subjective views or opinions that might be expressed in the paper do not necessarily represent the views of the U.S. Department of Energy or the U.S. Government. We would like to finally thank James J. Calvo and Annabelle Benin for assistance with sample preparation and Ryan Nishimoto for assistance with SEM measurements.

S.M.A., N.S.B., and M.C.S. carried out all synthesis and characterization. M.C.S. interpreted PXRD, SEM, Raman, DRS, UV, and conductivity data. M.E.F. performed and interpreted DFT calculations. V.N.S. collected and interpreted E.A. data. M.C.S. directed the project, as well as wrote and revised the manuscript with assistance from S.M.A. and N.S.B. A.A.T., V.N.S., and M.D.A. revised and polished the manuscript, as well as helped supervised the project. V.N.S. conceived the original idea.

Conflicts of interest

There are no conflicts to declare.

Notes and references

(1) Shiozawa, H.; Bayer, B. C.; Peterlik, H.; Meyer, J. C.; Lang, W.; Pichler, T. Doping of Metal–Organic Frameworks towards Resistive Sensing. *Sci. Rep.* **2017**, *7* (1), 2439. https://doi.org/10.1038/s41598-017-02618-y.

(2) Stassen, I.; Burtch, N.; Talin, A.; Falcaro, P.; Allendorf, M.; Ameloot, R. An Updated Roadmap for the Integration of Metal–Organic Frameworks with Electronic Devices and Chemical Sensors. *Chem. Soc. Rev.* **2017**, *46* (11), 3185–3241. https://doi.org/10.1039/C7CS00122C.

(3) Campbell, M.; Dincă, M. Metal–Organic Frameworks as Active Materials in Electronic Sensor Devices. *Sensors* **2017**, *17* (5), 1108. https://doi.org/10.3390/s17051108.

(4) So, M. C.; Jin, S.; Son, H.-J.; Wiederrecht, G. P.; Farha, O. K.; Hupp, J. T. Layer-by-Layer Fabrication of Oriented Porous Thin Films Based on Porphyrin-Containing Metal–Organic Frameworks. *J. Am. Chem. Soc.* **2013**, *135* (42), 15698–15701. https://doi.org/10.1021/ja4078705.

(5) Park, H. J.; So, M. C.; Gosztola, D.; Wiederrecht, G. P.; Emery, J. D.; Martinson, A. B. F.; Er, S.; Wilmer, C. E.; Vermeulen, N. A.; Aspuru-Guzik, A.; Stoddart, J. F.; Farha, O. K.; Hupp, J. T. Layer-by-Layer Assembled Films of Perylene Diimide- and Squaraine-Containing Metal–Organic Framework-like Materials: Solar Energy Capture and Directional Energy Transfer. *ACS Appl. Mater. Interfaces* **2016**, *8* (38), 24983–24988. https://doi.org/10.1021/acsami.6b03307.

(6) Yoon, S.; Talin, A. A.; Stavila, V.; Mroz, A. M.; Bennett, T. D.; He, Y.; Keen, D. A.; Hendon, C. H.; Allendorf, M. D.; So, M. C. From N- to p-Type Material: Effect of Metal Ion on Charge Transport in Metal–Organic Materials. *ACS Appl. Mater. Interfaces* **2021**, *13* (44), 52055–52062. https://doi.org/10.1021/acsami.1c09130.

(7) Calvo, J. J.; Angel, S. M.; So, M. C. Charge Transport in Metal–Organic Frameworks for Electronics Applications. *APL Mater.* **2020**, *8* (5), 050901. https://doi.org/10.1063/1.5143590.

(8) Allendorf, M. D.; Schwartzberg, A.; Stavila, V.; Talin, A. A. A Roadmap to Implementing Metal-Organic Frameworks in Electronic Devices: Challenges and Critical Directions. *Chem. - Eur. J.* **2011**, *17* (41), 11372–11388. https://doi.org/10.1002/chem.201101595.

(9) Zagorodniy, K.; Seifert, G.; Hermann, H. Metal-Organic Frameworks as Promising Candidates for Future Ultralow-k Dielectrics. *Appl. Phys. Lett.* **2010**, *97* (25), 251905. https://doi.org/10.1063/1.3529461.

(10) Yoon, S. M.; Warren, S. C.; Grzybowski, B. A. Storage of Electrical Information in Metal-Organic-Framework Memristors. *Angew. Chem. Int. Ed.* **2014**, *53* (17), 4437–4441. https://doi.org/10.1002/anie.201309642.

(11) Sheberla, D.; Sun, L.; Blood-Forsythe, M. A.; Er, S.; Wade, C. R.; Brozek, C. K.; Aspuru-Guzik, A.; Dincă, M. High Electrical Conductivity in Ni_3(2,3,6,7,10,11-Hexaiminotriphenylene)$_2$, a Semiconducting Metal–Organic Graphene Analogue. *J. Am. Chem. Soc.* **2014**, *136* (25), 8859–8862. https://doi.org/10.1021/ja502765n.

(12) Yamamoto, S.; Pirillo, J.; Hijikata, Y.; Zhang, Z.; Awaga, K. Nanopore-Induced Host–Guest Charge Transfer Phenomena in a Metal–Organic Framework. *Chem. Sci.* **2018**, *9* (13), 3282–3289. https://doi.org/10.1039/C7SC05390H.

(13) Clough, A. J.; Skelton, J. M.; Downes, C. A.; de la Rosa, A. A.; Yoo, J. W.; Walsh, A.; Melot, B. C.; Marinescu, S. C. Metallic Conductivity in a Two-Dimensional Cobalt Dithiolene Metal–Organic Framework. *J. Am. Chem. Soc.* **2017**, *139* (31), 10863–10867. https://doi.org/10.1021/jacs.7b05742.

(14) Sun, L.; Hendon, C. H.; Minier, M. A.; Walsh, A.; Dincă, M. Million-Fold Electrical Conductivity Enhancement in Fe_2(DEBDC) versus Mn_2(DEBDC) (E = S, O). *J. Am. Chem. Soc.* **2015**, *137* (19), 6164–6167. https://doi.org/10.1021/jacs.5b02897.

(15) Talin, A. A.; Centrone, A.; Ford, A. C.; Foster, M. E.; Stavila, V.; Haney, P.; Kinney, R. A.; Szalai, V.; El Gabaly, F.; Yoon, H. P.; Léonard, F.; Allendorf, M. D. Tunable Electrical Conductivity in Metal-Organic Framework Thin-Film Devices. *Science* **2014**, *343* (6166), 66–69. https://doi.org/10.1126/science.1246738.

(16) Schneider, C.; Ukaj, D.; Koerver, R.; Talin, A. A.; Kieslich, G.; Pujari, S. P.; Zuilhof, H.; Janek, J.; Allendorf, M. D.; Fischer, R. A. High Electrical Conductivity and High Porosity in a Guest@MOF Material: Evidence of TCNQ Ordering within Cu_3BTC_2 Micropores. *Chem. Sci.* **2018**, *9* (37), 7405–7412. https://doi.org/10.1039/C8SC02471E.

(17) Bláha, M.; Valeš, V.; Bastl, Z.; Kalbáč, M.; Shiozawa, H. Host–Guest Interactions in Metal–Organic Frameworks Doped with Acceptor Molecules as Revealed by Resonance Raman Spectroscopy. *J. Phys. Chem. C* **2020**, *124* (44), 24245–24250. https://doi.org/10.1021/acs.jpcc.0c07473.

(18) Zhou, W.; Wu, H.; Yildirim, T. Enhanced H_2 Adsorption in Isostructural Metal−Organic Frameworks with Open Metal Sites: Strong Dependence of the Binding Strength on Metal Ions. *J. Am. Chem. Soc.* **2008**, *130* (46), 15268–15269. https://doi.org/10.1021/ja807023q.

(19) Valenzano, L.; Civalleri, B.; Chavan, S.; Palomino, G. T.; Areán, C. O.; Bordiga, S. Computational and Experimental Studies on the Adsorption of CO, N_2, and CO_2 on Mg-MOF-74. *J. Phys. Chem. C* **2010**, *114* (25), 11185–11191. https://doi.org/10.1021/jp102574f.

(20) Poloni, R.; Lee, K.; Berger, R. F.; Smit, B.; Neaton, J. B. Understanding Trends in CO_2 Adsorption in Metal–Organic Frameworks with Open-Metal Sites. *J. Phys. Chem. Lett.* **2014**, *5* (5), 861–865. https://doi.org/10.1021/jz500202x.

(21) Tan, K.; Zuluaga, S.; Gong, Q.; Canepa, P.; Wang, H.; Li, J.; Chabal, Y. J.; Thonhauser, T. Water Reaction Mechanism in Metal Organic Frameworks with Coordinatively Unsaturated Metal Ions: MOF-74. *Chem. Mater.* **2014**, *26* (23), 6886–6895. https://doi.org/10.1021/cm5038183.

(22) Haldoupis, E.; Borycz, J.; Shi, H.; Vogiatzis, K. D.; Bai, P.; Queen, W. L.; Gagliardi, L.; Siepmann, J. I. Ab Initio Derived Force Fields for Predicting CO_2 Adsorption and Accessibility of Metal Sites in the Metal–Organic Frameworks M-MOF-74 (M = Mn, Co, Ni, Cu). *J. Phys. Chem. C* **2015**, *119* (28), 16058–16071. https://doi.org/10.1021/acs.jpcc.5b03700.

(23) Lee, K.; Howe, J. D.; Lin, L.-C.; Smit, B.; Neaton, J. B. Small-Molecule Adsorption in Open-Site Metal–Organic Frameworks: A Systematic Density Functional Theory Study for Rational Design. *Chem. Mater.* **2015**, *27* (3), 668–678. https://doi.org/10.1021/cm502760q.

(24) Jiang, H.; Wang, Q.; Wang, H.; Chen, Y.; Zhang, M. MOF-74 as an Efficient Catalyst for the Low-Temperature Selective Catalytic Reduction of NO_x with NH_3. *ACS Appl. Mater. Interfaces* **2016**, *8* (40), 26817–26826. https://doi.org/10.1021/acsami.6b08851.

(25) Strauss, I.; Mundstock, A.; Hinrichs, D.; Himstedt, R.; Knebel, A.; Reinhardt, C.; Dorfs, D.; Caro, J. The Interaction of Guest Molecules with Co-MOF-74: A Vis/NIR and Raman Approach. *Angew. Chem. Int. Ed.* **2018**, *57* (25), 7434–7439. https://doi.org/10.1002/anie.201801966.

(26) Strauss, I.; Mundstock, A.; Treger, M.; Lange, K.; Hwang, S.; Chmelik, C.; Rusch, P.; Bigall, N. C.; Pichler, T.; Shiozawa, H.; Caro, J. Metal–Organic Framework Co-MOF-74-Based Host–Guest Composites for Resistive Gas Sensing. *ACS Appl. Mater. Interfaces* **2019**, *11* (15), 14175–14181. https://doi.org/10.1021/acsami.8b22002.

(27) Boyd, R. H.; Phillips, W. D. Solution Dimerization of the Tetracyanoquinodimethane Ion Radical. *J. Chem. Phys.* **1965**, *43* (9), 2927–2929. https://doi.org/10.1063/1.1697251.

(28) Melby, L. R.; Harder, R. J.; Hertler, W. R.; Mahler, W.; Benson, R. E.; Mochel, W. E. **Substituted Quinodimethans. II. Anion-Radical Derivatives and Complexes of 7,7,8,8-Tetracyanoquinodimethan**. *J. Am. Chem. Soc.* **1962**, *84* (17), 3374–3387. https://doi.org/10.1021/ja00876a029.

(29) Foster, M. E.; Sohlberg, K.; Spataru, C. D.; Allendorf, M. D. Proposed Modification of the Graphene Analogue $Ni_3(HITP)_2$ To Yield a Semiconducting Material. *J. Phys. Chem. C* **2016**, *120* (27), 15001–15008. https://doi.org/10.1021/acs.jpcc.6b05746.

(30) Foster, M. E.; Sohlberg, K.; Allendorf, M. D.; Talin, A. A. Unraveling the Semiconducting/Metallic Discrepancy in $Ni_3(HITP)_2$. *J. Phys. Chem. Lett.* **2018**, *9* (3), 481–486. https://doi.org/10.1021/acs.jpclett.7b03140.

(31) Matsuzaki, S.; Kuwata, R.; Toyoda, K. Raman Spectra of Conducting TCNQ Salts; Estimation of the Degree of Charge Transfer from Vibrational Frequencies. *Solid State Commun.* **1980**, *33* (4), 403–405. https://doi.org/10.1016/0038-1098(80)90429-9.

(32) Kriebel, M.; Hennemann, M.; Beierlein, F. R.; Medina, D. D.; Bein, T.; Clark, T. Propagation of Holes and Electrons in Metal–Organic Frameworks. *J. Chem. Inf. Model.* **2019**, *59* (12), 5057–5064. https://doi.org/10.1021/acs.jcim.9b00461.

(33) Rosen, A. S.; Iyer, S. M.; Ray, D.; Yao, Z.; Aspuru-Guzik, A.; Gagliardi, L.; Notestein, J. M.; Snurr, R. Q. Machine Learning the Quantum-Chemical Properties of Metal–Organic Frameworks for Accelerated Materials Discovery. *Matter* **2021**, *4* (5), 1578–1597. https://doi.org/10.1016/j.matt.2021.02.015.

(34) Liu, L.; Dong, J.; Liu, J.; Liang, Q.; Song, Y.; Li, W.; Lei, S.; Hu, W. High-Quality Two-Dimensional Metal-Organic Framework Nanofilms for Nonvolatile Memristive Switching. *Small Struct.* **2021**, *2* (4), 2000077. https://doi.org/10.1002/sstr.202000077.

(35) Pollak, M. Effect of carrier-carrier interactions on some transport properties in disordered semiconductors. *Discuss. Faraday Soc.* **1970**, *50*, 13-19.

(36) Ambegaokar, V., Halperin, B.I. and Langer, J.S. Hopping conductivity in disordered systems. *Phys. Rev. B*, **1971**, *4(8)*, 2612-2620.

(37) Ohata, T.; Nomoto, A.; Watanabe, T.; Hirosawa, I.; Makita, T.; Takeya, J.; Makiura, R. Uniaxially Oriented Electrically Conductive Metal–Organic Framework Nanosheets Assembled at Air/Liquid Interfaces. *ACS Appl. Mater. Interfaces* **2021**, *13* (45), 54570–54578. https://doi.org/10.1021/acsami.1c16180.

(38) Scheurle, P. I.; Mähringer, A.; Biewald, A.; Hartschuh, A.; Bein, T.; Medina, D. D. MOF-74(M) Films Obtained through Vapor-Assisted Conversion—Impact on Crystal Orientation and Optical Properties. *Chem. Mater.* **2021**, *33* (15), 5896–5904. https://doi.org/10.1021/acs.chemmater.1c00743.

